Photoelectrochemistry of Composite Semiconductor Thin Films. Photosensitization of the SnO_2/TiO_2 Coupled System with a Ruthenium Polypyridyl Complex

Chouhaid Nasr,[†,‡] Prashant V. Kamat,[§] and Surat Hotchandani*[,†]

Groupe de Recherche en Énergie et Information Biomoléculaires, Université du Québec à Trois-Rivières, C.P. 500, Trois-Rivières, Québec G9A 5H7, Canada, and Radiation Laboratory, University of Notre Dame, Notre Dame, Indiana 46556

Received: July 14, 1998; In Final Form: September 28, 1998

In an effort to suppress charge recombination in nanoporous dye sensitized photoelectrochemical (DSPE) solar cells, nanocrystalline coupled semiconductor electrodes of the type OTE/SnO_2/TiO_2 have been prepared, and their photosensitization with a ruthenium polypyridyl complex, Ru(II), has been carried out (OTE is an optically transparent electrode). Improved photoresponse, i.e., higher incident photon to current conversion efficiency (IPCE), higher photovoltage, lower back-electron-transfer rate, k_r, and similar front- and back-face action spectra in the coupled OTE/SnO_2/TiO_2/Ru(II) system compared to those for simple OTE/SnO_2/Ru(II) and OTE/TiO_2/Ru(II) ones emphasize the potential of a coupled electrode in bringing about an efficient charge separation in nanocrystalline DSPE cells. A negligible photocurrent in a reverse composite OTE/TiO_2/SnO_2/Ru(II) system underscores the importance of the proper placement of the energy levels of individual semiconductor components in the coupled system for vectorial electron transfer to ameliorate charge separation. The results of the variation of IPCE in the coupled OTE/SnO_2/TiO_2/Ru(II) system, where IPCE initially increases but later decreases as the thickness of the TiO_2 film further increases, suggest an interplay between the forces of charge separation and charge recombination. The increase of IPCE is, of course, due to the better charge separation ability of the coupled system while the decrease points to the increased charge recombination losses. Similar arguments have also been put forth to explain the behavior of the back-electron-transfer rate with the thickness of TiO_2 film in the coupled system.

Introduction

Photoelectrochemical solar cells based on the photosensitization of thin semiconductor films with inorganic[1−7] and organic dyes[8−13] have regained a considerable interest after Grätzel and co-workers reported a power conversion efficiency of as high as 11−15% in diffuse daylight for a solar cell based on a ruthenium complex adsorbed on highly porous nanocrystalline TiO_2 films.[4] The key elements of their cell are the large surface area and high porosity of the nanocrystalline semiconductor films. As a result, these films enhance the light-harvesting capability of the pigment adsorbed on them and also allow the penetration of the electrolyte right up to the supporting electrode that aids in charge separation process, thus leading to a high power conversion efficiency of the cell (for reviews please refer to Lampert,[14] Kamat,[15] and Hagfeldt and Grätzel[16]).

A rather unusual feature of these nanocrystalline films based solar cells, however, is the lack of the depletion layer at the semiconductor/electrolyte interface.[17−20] As a result, the back electron transfer, i.e., the charge recombination between the electrons injected in the conduction band of the semiconductor and the oxidized sensitizer, still remains one of the major limiting factors to the efficiency of the cells. The use of a redox couple in the electrolyte does prevent the back electron transfer to some extent as it quickly donates its electron to the oxidized sensitizer to regenerate the original sensitizer. The charge recombination can further be slowed by the application of an external bias, however, for commercial and practical viability of solar energy conversion, such a configuration is less appealing and undesirable.

A simple and elegant approach to suppress the back electron transfer is to produce a long-distance charge-separated state, with electrons and holes at sites far from each other, through the use of coupled, i.e., the combination of two or more, semiconductors with appropriate energy levels.[21−24] In these coupled systems, for instance, ZnO/CdS, the energy levels of the semiconductors are such that the electrons photogenerated or injected in CdS are quickly transferred to the lower lying conduction band of ZnO.[21] As a result, the electrons and holes are physically separated, thus reducing the possibility of back electron transfer and suppressing the wasteful charge recombination.

Various studies from our laboratory and elesewhere have shown an improved photocurrent generation in nanocrystalline coupled semiconductor films of TiO_2/CdS,[25−27] ZnO/CdS,[21] TiO_2/CdSe,[28] and SnO_2/CdSe.[29] Vogel et al.[30] have recently reported a photoelectrochemical study of several semiconductor systems obtained by coupling large band gap semiconductors TiO_2, Nb_2O_5, ZnO, TiO_2, and SnO_2 with small band gap semiconductors CdS, Bi_2S_3, Ag_2S, and PbS. A better charge separation in the coupled systems is the result of fast electron-transfer process between the two semiconductors. We have shown that the charge injection process in ZnO/CdS system occurs within the pulse duration of the laser (20 ps).[21] A recent study by Evans et al.[31] has indicated that the interparticle

* To whom correspondence should be addressed. E-mail: hotchand@uqtr.uquebec.ca.
[†] Université du Quebéc à Trois-Rivières.
[‡] E-mail: nasr@uqtr.uquebec.ca.
[§] University of Notre Dame. E-mail: pkamat@nd.edu.

10.1021/jp983021c CCC: $15.00
Published on Web 11/13/1998

electron transfer in the coupled TiO_2/CdS system has a time constant of 2 ps.

With the dye or sensitizer adsorbed on such a coupled system, e.g., ZnO/CdS, the photogenerated electrons in the dye rapidly find their way to the lower lying conduction band of ZnO while holes remain on the dye, farther from the electrons.[32] The increased photocurrent generation in chlorophyll a (Chl a) deposited on ZnO/CdS coupled eletrode compared to that with Chl a adsorbed on ZnO alone lends support to the enhanced charge separation with coupled system.[32] Vinodgopal et al. also reported a 10 times enhancement in the photocatalytic degradation rates of several textile azo dyes, as a result of better charge separation, using an SnO_2/TiO_2 composite systems.[33] Various other composite systems such as TiO_2/CdS, TiO_2/WO_3, TiO_2/MnO_2, TiO_2/SiO_2, and TiO_2/ZrO_2 have also been found useful in enhancing the rates of photocatalytic degradation processes.[33−40]

In a more recent work,[41] we reported a detailed study to highlight the usefulness of a composite SnO_2/CdS electrode in dye sensitization experiments with a ruthenium polypyridyl complex, hereafter abbreviated as Ru(II). A higher photoconversion efficiency and a lower back-electron-transfer rate were, indeed, observed with Ru(II) adsorbed on a coupled OTE/SnO_2/CdS electrode, i.e., the system OTE/SnO_2/CdS/Ru(II), compared to the OTE/SnO_2/Ru(II) one in which Ru(II) was deposited on simple OTE/SnO_2 electrode. (OTE is an optically transparent electrode on which various components are sequentially deposited from left to right; the details are in the Experimental Section.) These results were ascribed to the better charge separation ability of the coupled electrode.

From a scientific standpoint and to further prove our point with regard to the better charge separation with the coupled electrode, it would have been instructive to demonstrate that the coupled system OTE/SnO_2/CdS/Ru(II) also fared better than OTE/CdS/Ru(II) and OTE/CdS/SnO_2/Ru(II) systems in which Ru(II) was, respectively, deposited on a simple OTE/CdS electrode and reverse coupled OTE/CdS/SnO_2 electrodes. In the latter, the energy levels of the two semiconductors, constituting the coupled electrode, are in reverse and unfavorable order for electron transfer. This, however, was not possible as good nanocrystalline OTE/CdS electrodes by depositing nanometer-sized CdS colloidal particles directly on bare OTE could not be prepared. Due to this difficulty encountered, the reverse coupled OTE/CdS/SnO_2 electrodes (semiconductors with energy levels in reverse order) could also not be prepared. Furthermore, conduction band, E_{CB}, of CdS (~-0.8 V vs NHE) and the oxidation potential, $E°$, of excited Ru(II), ~-0.75 V vs NHE,[41] are very close to each other, thus providing virtually zero or no driving force for photoinduced electron transfer from excited Ru(II), Ru(II)*, to CdS. Consequently, the full impact of the coupled SnO_2/CdS electrode in improving charge separation in Ru(II) might not have been realized.

We, therefore, decided to extend the above work by replacing CdS with TiO_2, i.e., to fabricate the coupled systems of SnO_2 and TiO_2 nanocrystalline films, and study their photosensitization with Ru(II). It should be noted that E_{CB} of TiO_2 (-0.5 V vs NHE)[42] is decidedly lower in energy than the $E°$ of Ru(II)* but is, at the same time, definitely superior in energy to E_{CB} of SnO_2 (0 V vs NHE),[41] thereby rendering the flow of electrons from Ru(II)* to TiO_2 to SnO_2 a barrierless process. Moreover, since TiO_2 particles could easily be deposited on OTE, the assembly of simple OTE/TiO_2 and reverse coupled OTE/TiO_2/SnO_2 electrodes posed no problems. The utility of the reverse composite OTE/TiO_2/SnO_2 electrode, with conduction band of TiO_2 being at higher energy than that of SnO_2, is that it will provide a testing ground for the crucial criterion of proper positioning of the energy levels of individual semiconductors in a coupled system for efficient electron transfer.

A preliminary account of the sensitization of coupled SnO_2/TiO_2 electrodes with Ru(II) has recently been reported.[43] However, these electrodes were prepared from the mixture of colloidal SnO_2 solution and a slurry of TiO_2 powder (Degussa P25), and as a result, the SnO_2 and TiO_2 particles were rather randomly distributed on the electrode. In the present study, TiO_2 employed is also in colloidal solution form, and the electrodes have been prepared by sequentially depositing the individual nanocrystalline films of SnO_2 and TiO_2 on OTE in particular and specific order. Further, the thickness of semiconductor films has also been varied to examine its effect on the photocurrent generation and back-electron-transfer processes. We present in this paper a detailed study of photoelectrochemical and time-resolved flash photolysis experiments of various Ru(II) modified electrodes, i.e., the systems OTE/SnO_2/Ru(II), OTE/TiO_2/Ru(II) and OTE/SnO_2/TiO_2/Ru(II), to illustrate the beneficial role of coupled semiconductor system in charge separation and improving the performance of dye-sensitized photoelectrochemical (DSPE) solar cells.

Experimental Section

Materials. Optically transparent electrodes (OTE) were cut from an indium tin oxide coated glass plate (1.3 mm thick, 20 Ω/square) obtained from Donelley Corp., Holland, MI. The SnO_2 colloidal suspension (15%, particle diameter 10−15 nm) was obtained from Alfa Chemicals and was used without further purification. TiO_2 colloidal solution was prepared by following the procedure developed by Gregg and co-workers,[44] which is a variant of the original one reported by Grätzel and co-workers.[4] Briefly, the method consists of adding dropwise a mixture of 37 mL of Ti(IV) isopropoxide (Aldrich, 99.9%) and 10 mL of 2-propanol to a stirred solution of glacial acetic acid (80 mL) in 250 mL of dionized water over a period of 30 min. Stirring was continued for 4−6 h at 353 K, and the resulting solution was transferred to a well-sealed autoclave vessel and additionally heated for 12 h at 503 K. Excess water was then removed by rotary evaporation until a TiO_2 concentration of 120 g/L was obtained.

Absorption spectra were recorded with a Milton Roy Spectronic diode array spectrophotometer.

Preparation of SnO_2 Particulate Films. The procedure of casting transparent thin films of SnO_2 on an optically transparent electrode (OTE) has been reported previously.[1] A small aliquot (usually 0.75 mL) of SnO_2 colloidal suspension (0.15%) was applied to the conducting surface of 0.8×5 cm^2 of OTE and was dried in air on a warm plate. The SnO_2 colloid-coated OTE was then annealed for 1 h at 673 K. This electrode will be referred to as OTE/SnO_2 electrode.

Preparation of OTE/TiO_2 and Coupled OTE/SnO_2/TiO_2 Electrodes. These electrodes were prepared by spin coating the desired amount of TiO_2 colloidal solution on OTE and OTE/SnO_2 electrodes at 2000 rpm, respectively, followed by annealation at 673 K for 1 h. The reverse coupled OTE/TiO_2/SnO_2 electrode was prepared by deposition of SnO_2 particulate film on OTE/TiO_2 substrate as described above for OTE/SnO_2 electrodes.

Modification of the Electrodes with Ru(2,2′-bipyridine)$_2$-(2,2′-bipyridine-4,4′-dicarboxylic acid)$^{2+}$. The above nanocrystalline electrodes were modified with Ru(2,2′-bipyridine)$_2$-(2,2′-bipyridine-4,4′-dicarboxylic acid)$^{2+}$, referred to as Ru(II) in the text, by dipping them directly in an acetonitrile solution

of Ru(II), $\sim 10^{-3}$ M, for a period of 8−10 h. The electrode was then thoroughly washed with acetonitrile and stored in the dark. The deepening of an orange coloration of the nanoporous semiconductor film confirmed the adsorption of Ru(II) in large amounts. These Ru(II)-modified electrodes will be denoted as simple OTE/SnO_2/Ru(II), OTE/TiO_2/Ru(II), coupled OTE/SnO_2/TiO_2/Ru(II), and reverse coupled OTE/TiO_2/SnO_2/Ru(II) systems in the following discussion.

Photoelectrochemical Measurements. The measurements were carried out in a thin layer cell consisting of a 2 or 5 mm path length quartz cuvette with two sidearms attached for inserting reference (Ag/AgCl) and counter (Pt gauze) electrodes. A solution of 0.04 M I_2 and 0.5 M LiI in acetonitrile was used as electrolyte. Photocurrent measurements were made with a Keithley model 617 programmable electrometer. A collimated light beam from a 250 W xenon lamp was used as the light source. A Bausch and Lomb high-intensity grating monochromator was introduced into the path of the excitation beam for selecting the excitation wavelength.

Laser Flash Photolysis Experiments. The spectroelectrochemical cell containing the Ru(II) modified electrode was placed in the sample compartment of the nanosecond laser flash photolysis setup. The excitation was carried out in a front face geometry with 532 nm laser pulses from a Quanta-Ray CDR-1 Nd:YAG laser system (~6 ns pulse width, 5 mJ). The laser output was suitably attenuated to ~ 1 mJ/pulse to minimize the occurrence of multiphoton processes. The photomultiplier output was digitized with a Tektronix 7912 AD programmable digitizer. A typical experiment consisted of a series of 3−6 replicate shots per single measurement. The average signal was processed with an LSI-11 microprocessor interfaced with a VAX computer.[45]

In all these experiments, unless otherwise stated, the thickness of SnO_2 film was ~0.75 μm, the active area of the electrode was 1 cm^2, and the illumination of the electrodes was through the back OTE face. The thickness of TiO_2 film was varied by spin coating the varying amounts of TiO_2 solution on the electrodes; the thickness of the films was measured with a profilometer (alpha step 200, Tencor Instruments).

Results

A. Absorption and Photoelectochemical Properties of OTE/SnO_2, OTE/TiO_2, and OTE/SnO_2/TiO_2 Electrodes. The absorption spectra of the electrodes are shown in Figure 1A. The SnO_2 and TiO_2 film coated electrodes absorb in the UV with an absorption below 360 and 400 nm, respectively, which correspond to their absorption edges ($E_g(SnO_2) = 3.6$ eV) and ($E_g(TiO_2) = 3.2$ eV). The OTE/SnO_2/TiO_2 electrode, on the other hand, shows the same absorption profile as that for TiO_2 electrode but with increased absorption.

Short-circuit photocurrents (I_{sc}) were measured at various excitation wavelengths (λ), and incident photon to current conversion efficiency (IPCE) was determined from the following expression:[21]

$$\text{IPCE (\%)} = \frac{I_{sc}\ (\text{A/cm}^2)}{I_{inc}\ (\text{W/cm}^2)} \times \frac{1240}{\lambda\ (\text{nm})} \times 100 \qquad (1)$$

where I_{inc} is the light incident on the electrode. The electrolyte used was a 0.02 M aqueous NaOH solution.

The action spectra, representing IPCE vs λ, of the electrodes are shown in Figure 1B. The respective onsets of photocurrent are seen at 360 nm for SnO_2 and 400 nm for TiO_2 and SnO_2/TiO_2 electrodes and match well their absorption characteristics

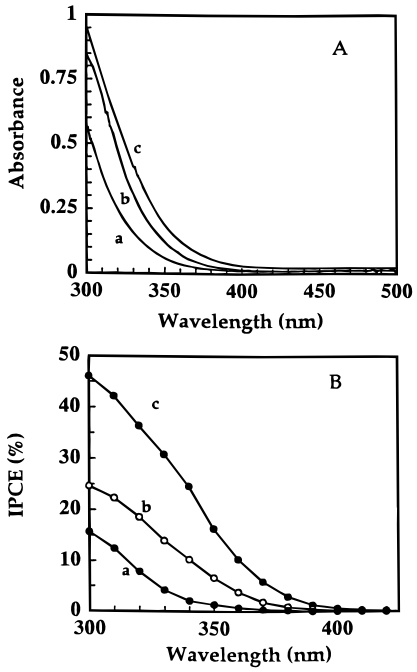

Figure 1. (A) Absorption and (B) photocurrent action spectra of (a) OTE/SnO_2, (b) OTE/TiO_2, and (c) OTE/SnO_2/TiO_2 electrodes. The respective thicknesses of the films are $SnO_2 = 0.75$ μm and $TiO_2 = 0.75$ μm for electrodes a and b, while those for the coupled electrode c are $SnO_2 = 0.75$ μm and $TiO_2 = 0.25$ μm. For IPCE measurements, electrolyte employed is 0.02 M aqueous NaOH.

shown in Figure 1A. This indicates that the photocurrent is generated by the excitation of the nanocrystalline particles. An important feature is that the coupled OTE/SnO_2/TiO_2 electrode shows an almost double and triple IPCE compared to TiO_2 and SnO_2 electrodes, respectively. This confirms that a better charge separation occurs in the coupled electrode. The generation of an anodic photocurrent suggests that the flow of the electrons is toward the OTE surface. It should be noted that the increase in IPCE for the coupled electrode cannot be attributed to an increase in the absorption of light as a result of greater thickness of the electrode. To remove this ambiguity, IPCEs of simple SnO_2 and TiO_2 electrodes, each with same thickness (1 μm) as that of the coupled electrode, were measured. In both cases, the increase in IPCEs was only 10−15%, confirming, therefore, the beneficial role of the coupling.

B. Ru(II)-Modified Nanocrystalline Semiconductor Electrodes. *(I) Absorption Characteristics.* Following the adsorption of Ru(II), the OTE/SnO_2, OTE/TiO_2, and OTE/SnO_2/TiO_2 electrodes exhibited strong absorption in the visible, with a maximum around 460−470 nm, confirming the binding of the sensitizer to the semiconductor surface. Figure 2 displays a typical spectrum of the coupled OTE/SnO_2/TiO_2 electrode before and after its modification with Ru(II); similar spectra were also obtained with other Ru(II)-modified electrodes. It has been suggested by Gratzel and co-workers,[4] and later verified by Murakoshi *et al.*[3] by detailed UV and IR spectroscopic measurements, that the carboxylic group of Ru(II) forms an ester-like or carboxylato linkage with titanium or tin atoms on TiO_2 or SnO_2 nanocrystallites, respectively, and is responsible for the strong adsorption of Ru(II) on the TiO_2 or SnO_2 surface.

We also followed the evolution of the absorbance of Ru(II) at 460 nm with the thickness of TiO_2 film in the coupled system

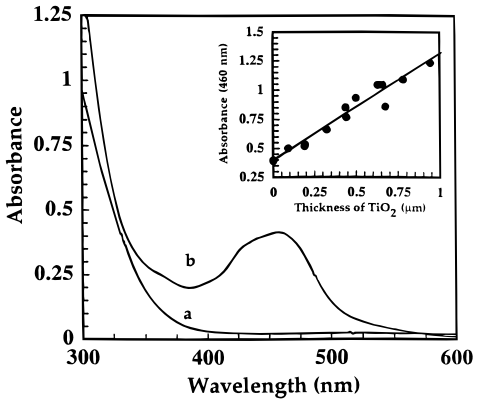

Figure 2. Absorption spectra of OTE/SnO_2/TiO_2 electrode (a) before and (b) after modification with Ru(II). The inset shows the absorbance of OTE/SnO_2/TiO_2/Ru(II) system at 460 nm with varying thickness of TiO_2 film. The thickness of SnO_2 film was kept constant at 0.75 μm, and zero thickness of TiO_2 film refers to OTE/SnO_2/Ru(II).

(please note that the zero thickness of TiO_2 film refers to the OTE/SnO_2/Ru(II) system); the result is shown in the inset of Figure 2. The increase in thickness of TiO_2 film results in an increase in the absorbance of Ru(II). This is understandable in view of the fact that the greater is the thickness of the supporting film, the greater is the adsorption of the dye and, therefore, the greater is its capacity to harvest the incident light. No saturation in absorption was observed up to 1 μm thickness of TiO_2 film. Similar absorption characterstics were also observed with increase in SnO_2 film thickness.

(II) Photoelectrochemical Behavior. In our earlier study, we have shown that Ru(II)-modified SnO_2 nanocrystalline semiconductor films exhibit excellent electrochemical and photoelectrochemical properties.[1,41] This is due, in part, to the high porosity of the SnO_2 film which facilitates larger uptake of the dye and, in part, to the presence of carboxylic group in Ru(II), which, besides aiding in the stronger adsorption of Ru(II), also assists in electron-transfer process as a result of increased electronic coupling between π*-orbitals of Ru(II)* and conduction manifold of the semiconductor. In the following, we describe various photoelectrochemical characterstics of simple and coupled electrodes modified with Ru(II). It should be noted that in all these experiments, a 400 nm cutoff filter was employed to block the direct UV band gap excitation of SnO_2 and TiO_2 nanocrystalline semiconductors.

(a) Photocurrent Action Spectra. The photocurrent responses of simple OTE/SnO_2/Ru(II), OTE/TiO_2/Ru(II), and coupled OTE/SnO_2/TiO_2/Ru(II) systems are shown in Figure 3. All these systems show maximum photocurrent around 460−470 nm which corresponds to the absorption maximum of Ru(II). The qualitative matching of the action and absorption spectra of the modified electrodes suggests that the photosensitization mechanism is operative in generation of photocurrent. Briefly, upon excitation with visible light (absorbed predominantly by Ru(II)), excited Ru(II), Ru(II)*, injects electrons in semiconductor particles which are then collected at the back OTE contact to generate an anodic photocurrent. The electron donor, for example iodide, in the electrolyte helps quickly regenerate the original sensitizer thus preventing the wasteful charge recombination. The interaction of iodide with Ru(II) adsorbed on SnO_2 and SiO_2 films was the subject of a recent work.[46] The process of generation of sensitized photocurrent in an OTE/

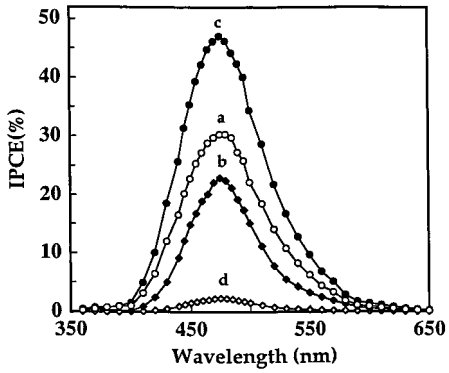

Figure 3. Photocurrent action spectra of (a) OTE/SnO_2/Ru(II), (b) OTE/TiO_2/Ru(II), (c) coupled OTE/SnO_2/TiO_2/Ru(II), and (d) reverse coupled OTE/TiO_2/SnO_2/Ru(II) systems with illumination through OTE (electrolyte: 0.04 M I_2 and 0.5 M LiI in acetonitrile). The thicknesses of the semiconductor films for systems a and b are SnO_2 = 0.75 μm and TiO_2 = 0.75 μm, respectively, while those for systems c and d are respectively SnO_2 = 0.75 μm, TiO_2 = 0.25 μm and TiO_2 = 0.75 μm, SnO_2 = 0.75 μm.

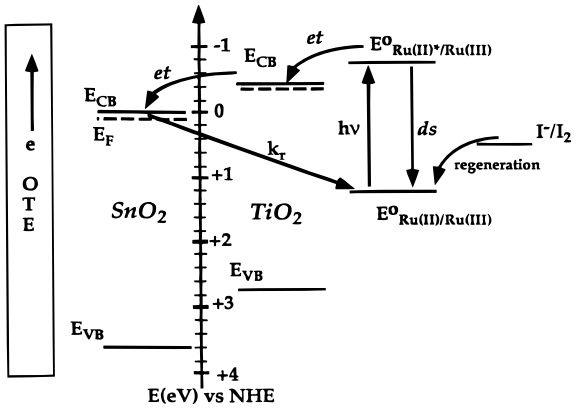

Figure 4. Energy level diagram illustrating the conduction band (CB) and valence band (VB) of SnO_2 and TiO_2, and redox potentials (E°) of ground and excited states of Ru(II) and of redox couple I^-/I_3^-. The processes ds and et represent respectively the deactivation of Ru(II)* to the ground state and electron transfer, while k_r is the back-electron-transfer rate constant.

SnO_2/TiO_2/Ru(II) composite system is described as follows and is depicted in Figure 4.

$$\mathrm{Ru(II)} + h\nu \rightarrow \mathrm{Ru(II)^*} \quad (2)$$

$$\mathrm{Ru(II)^*} \xrightarrow{\mathrm{ds}} \mathrm{Ru(II)} \quad (3)$$

$$\mathrm{Ru(II)^* + SnO_2/TiO_2} \xrightarrow{\mathrm{et}} \mathrm{SnO_2/TiO_2(e) + Ru(III)} \xrightarrow{\mathrm{et}} \mathrm{SnO_2(e)/TiO_2 + Ru(III)} \quad (4)$$

$$\mathrm{2Ru(III) + 3I^-} \xrightarrow{\mathrm{regen}} \mathrm{2Ru(II) + I_3^-} \quad (5)$$

$$\mathrm{Ru(III) + SnO_2(e)/TiO_2} \xrightarrow{k_r} \mathrm{Ru(II) + SnO_2/TiO_2} \quad (6)$$

where ds, et, and regen are, respectively, the processes of deactivation of Ru(II)* to the ground state, electron transfer, and regeneration of the sensitizer, while k_r is the rate constant for back electron transfer.

The beneficial role of coupling is at once evidenced if one compares the action spectra of the systems. Clearly, the IPCE with a coupled electrode is much superior. A nearly 50% and 100% increase in IPCE at 460 nm can easily be noticed in composite OTE/SnO_2/TiO_2/Ru(II) system in comparison with simple OTE/SnO_2/Ru(II) and OTE/TiO_2/Ru(II) ones, respec-

tively. This surely suggests an improved charge separation brought about by the coupled electrode. While, in all these systems, some of the photogenerated charges are lost by recombination, the charge recombination is much less in the coupled system than in the simple SnO_2/Ru and TiO_2/Ru(II) systems. The explanation is that in the coupled system, the electrons injected from Ru(II)* ($E^\circ = -0.75$ V vs NHE) into TiO_2 ($E_{CB} = -0.5$ V vs NHE) quickly migrate to the lower lying conduction band of SnO_2 ($E_{CB} = 0$ V vs NHE). As a result, they are farther apart from the holes left in Ru(II), i.e., the oxidized form Ru(III), and escape recombination and are collected in greater number at the back contact OTE producing a larger photocurrent. Similar observations have earlier been made with SnO_2/CdS and ZnO/CdS coupled electrodes in their sensitization with Ru(II) and Chl a, respectively.[32,41]

To ensure that the enhanced photoresponse in coupled system was, indeed, due to the vectorial transfer of electrons from TiO_2 to SnO_2 particles and not merely due to the increased light harvesting efficiency (LHE) of Ru(II) resulting from its adsorption on the thicker coupled electrode, IPCEs of simple OTE/SnO_2/Ru(II) and OTE/TiO_2/Ru(II) systems, with thickness of SnO_2 and TiO_2 films each equal to that of the coupled electrode (1 μm), were measured. The IPCEs did increase but only by ~10%; i.e., IPCEs remained much lower than that for the coupled system. Further, after deposition of the thin (0.2 μm) TiO_2 film on SnO_2 film (0.75 μm), the increase in LHE ($=1 - 10^{-A}$) of Ru(II), as seen from the inset of Figure 2, is only ~12%, whereas the increase in IPCE of coupled system relative to the OTE/SnO_2/Ru(II) and OTE/TiO_2/Ru(II) systems, as mentioned above, is ~50 and 100%, respectively. This suggests that the increase in IPCE of the coupled system is really due to the cascading of electrons from TiO_2 to SnO_2 leading to a better process of charge separation.

To give further credence to the importance of the vectorial nature of the electron transfer in the coupled system, the IPCE of a reverse coupled system, OTE/TiO_2/SnO_2/Ru(II), i.e., Ru(II) deposited on the OTE/TiO_2/SnO_2 electrode, in which the ordering of the energy levels of SnO_2 and TiO_2 is reversed, was also measured. In this case, the theory suggests that the electrons injected from Ru(II)* into the conduction band of SnO_2, in view of the negative driving force created by the unfavorable positioning of the energetic bands of the two semiconductors, should not migrate to the higher lying conduction band of TiO_2 and, thus, should not reach the back contact; with the result the sensitized photocurrent response should be nil. As noticed in curve d (Figure 3), which presents the action spectrum of the reverse coupled OTE/TiO_2/SnO_2/Ru(II) system, this, indeed, is the case. The photocurrent is practically negligible, even though the uptake of Ru(II) is reasonably high (absorbance at 460 nm is ~0.8). This validates and proves that the proper placement of energy levels in coupled systesm is, indeed, crucial for efficient electron transfer.

It should, however, be mentioned that, in reverse coupled systems with thin (~0.2 μm) films of SnO_2, inspite of the thermodynamic barrier, a nonnegligible photocurrent was, nevertheless, observed. This is most likely the result of some of Ru(II) molecules that were able to penetrate the highly porous SnO_2 film and got adsorbed on TiO_2 particles. In this case, Ru(II)* injected electrons directly into the conduction band of TiO_2 which were then collected at the back contact to produce photocurrent. The thicker SnO_2 films, however, hamper the passage of Ru(II) molecules through SnO_2 pores and prevent their direct adsoption on TiO_2 film.

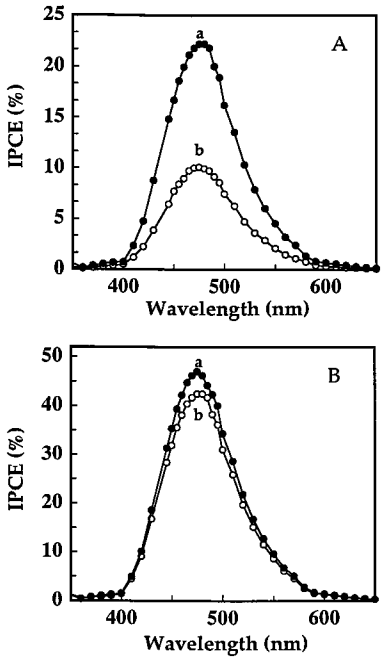

Figure 5. Photocurrent action spectra of (A) simple OTE/TiO_2/Ru(II) and (B) coupled OTE/SnO_2/TiO_2/Ru(II) systems for back face (a) and front face (b) illumination modes (electrolyte: 0.04 M I_2 and 0.5 M LiI in acetonitrile). The thickness of the semiconductor films are as described in Figure 3.

(b) Dependence of IPCE with Side of Illumination. The illumination of the cell, i.e., through electrolyte or front face (FF) or through the substrate OTE or back face (BF), plays an important role in recombination losses suffered by the electrons injected in the nanocrystalline semiconductor films and, hence, in the photogeneration of the current. Figure 5A presents the action spectra of simple OTE/TiO_2/Ru(II) system for FF and BF illuminations. One notices a larger photocurrent for BF illumination. Similar observations have also been reported by other researchers.[19,47,48] This behavior has been explained on the basis of the different distances that the electrons injected from the dye have to travel in the semiconductor films to reach the collecting back electrode to produce current in the external circuit for the two modes of illumination.

It has been shown that the most efficient charge separation in nanoporous cells occurs close to the back OTE electrode[1,19,47] and that the pronounced differences in action spectra are observed with the thicker films.[19a] Sodergren et al.,[19b] further developed a theoretical model which correctly describes the salient features of the action spectra for both BF and FF illuminations for bare and dye-modified nanocrystalline films. According to this model, which assumes the electron transport in nanoporous cells to occur via diffusion, the closer the electrons injected in the semiconductor are to the back OTE contact, the lesser is the probability of their recombination with the holes during their voyage to the collecting back electrode. Thus, in the case of BF illumination (spectrum a, Figure 5A), most of the electrons injected in TiO_2 particles are in close vicinity of the back contact and are collected with high efficiency to produce a larger photocurrent. In the case of FF illumination, on the other hand, the charge injection, especially for strongly absorbing wavelengths, occurs farther away from the back OTE contact. Consequently, the probability of collection diminishes and smaller photocurrent is generated. Similar behavior was also seen with the simple OTE/SnO_2/Ru(II) electrodes; the results are summarized in Table 1.

TABLE 1: Incident Photon-to-Current Conversion Efficiency (IPCE) and Maximum Photovoltage, V_{oc}, and Back Electron Transfer, k_r, of Ru(II) Complex Adsorbed on Different Nanocrystalline Semiconductor Electrodes

systems	IPCE (%)[a] back face	IPCE (%) front face	V_{oc} (mV) back face	k_r (10^6 s^{-1})
simple OTE/SnO_2/Ru(II)[b]	30	15	300	1.2
simple OTE/TiO_2/Ru(II)[c]	22	10	550	2.3
coupled OTE/SnO_2/TiO_2/ Ru(II) with thin TiO_2 film[d]	46	44	400	0.4
coupled OTE/SnO_2/TiO_2/ Ru(II) with thick TiO_2 film[e]	25	12		2

[a] IPCE (%) was determined according to eq 1. [b] Thickness of the SnO_2 film is 0.75 μm. [c] Thickness of the TiO_2 film is 0.75 μm. [d] Thickness of the SnO_2 film is 0.75 μm, and that of TiO_2 is 0.2 μm. [e] Thickness of the SnO_2 film is 0.75 μm, and that of TiO_2 film is 0.75 μm.

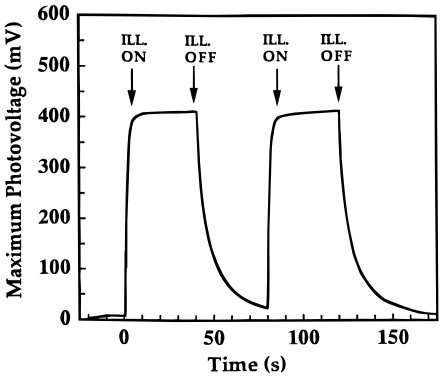

Figure 6. Open-circuit photovoltage response of OTE/SnO_2/TiO_2/Ru-(II) system to visible light (460 nm) with BF illumination (electrolyte: 0.04 M I_2 and 0.5 M LiI in acetonitrile).

The picture that emerges from the coupled OTE/SnO_2/TiO_2/Ru(II) system is, however, quite different (Figure 5B). The photocurrent obtained with both modes of illumination is, surprisingly, almost comparable. As a matter of fact, owing to the increased semiconductor film thickness in the coupled system, the intuition dictates that the photocurrent for FF mode of illumination be much smaller. However, the results show otherwise. We believe that the rapid transfer of electrons from TiO_2 to the lower lying conduction band of SnO_2, which produces electrons and holes farther from each other (electrons in SnO_2 and holes left in ruthenium), is responsible for these unexpected results. Thus, in the case of FF illumination where charge injection takes place in outer layers away from the back contact, the very phenomenon of electrons rapidly finding themselves in SnO_2, away from the holes, enables them to travel safely even the greater distances and arrive at the collecting electrode incurring smaller recombination losses and yield as much photocurrent as that with BF illumination. This aspect, once again, underlines the importance of the proper placement of energy levels in the coupled system for better charge separation.

(c) Photovoltage Response. The generation of photovoltage in simple and coupled electrodes was prompt and was reproducible for several on−off cycles of illumination. A representative curve for photovoltage response of coupled OTE/SnO_2/TiO_2/Ru(II) system is shown in Figure 6. Upon illumination, the photogenerated electrons in the dye are quickly transferred to the conduction band of the semiconductor. Consequently, the Fermi level of the semiconductor moves very close to the conduction band, and the maximum photovoltage that one can obtain is the energy difference between the conduction band of the semiconductor and the oxidation potential of the redox couple present in the electrolyte. Taking into consideration the E_{ox} of the redox couple (I_3^-/I^-) $\sim$ 0.5 V vs NHE[49] and the reported values of E_{CB} for SnO_2 (0.0 V vs NHE) and TiO_2 (−0.5 V vs NHE), the simple OTE/SnO_2/Ru(II) and OTE/TiO_2/Ru-(II) systems should furnish maximum photovoltage, V_{oc}, of 500 and 1000 mV, respectively. The actual values obtained, however, as shown in Table 1, are respectively 300 and 550 mV and are smaller than the theoretical predicted values. This is most likely due to the charge recombination losses.

In the coupled system, OTE/SnO_2/TiO_2/Ru(II), since the final electron acceptor is SnO_2, the maximum photovoltage obtained will also be the energy difference between conduction band of SnO_2 and the oxidation potential of the electrolyte. Thus, one would expect the coupled system to essentially behave as simple OTE/SnO_2/Ru(II) system as far as the V_{oc} is concerned and yield a V_{oc} of $\sim$ 300 mV. As noted from Figure 6 and Table 1, V_{oc} of 400 mV for the coupled system is superior to that for simple one. This strongly suggests that the recombination losses in coupled system are occurring to a lesser degree and is the direct result of the quick cascading of electrons from TiO_2 to SnO_2. Once again to verify that a higher V_{oc} in the coupled system was not due to the increased semiconductor thickness and, hence, the increased LHE of Ru(II), V_{oc}s of simple OTE/SnO_2/Ru(II) and OTE/TiO_2/Ru(II) systems, with SnO_2 and TiO_2 film thickness each equal to that of the coupled semiconductor, were measured. These values were, within the experimental error, very close to the ones shown in Table 1 for simple systems. This, indeed, is very encouraging and gratifying and reinforces our very basic strategy of the utility of the coupled system with appropriate energy levels to enhance the charge separation and improve the performance of DSPE cells.

(d) Dependence of IPCE with the Thickness of TiO_2 Film. Since it is in the TiO_2 film that the injection of electrons from Ru(II)* primarily occurs and since it is also from TiO_2 that the cascading of electrons to SnO_2 starts, it is of great interest to examine how the thickness of the TiO_2 film will control the electron flow from TiO_2 to SnO_2 and affect the photocurrent generation in the coupled system. Once in SnO_2, the electrons are already farther away from holes, and as a result, the thickness of the SnO_2 film plays a less critical role in charge transport and, hence, in photocurrent output of the coupled system.

The variation of IPCE, measured at 460 nm for OTE/SnO_2/TiO_2/Ru(II) system, with TiO_2 thickness is presented in Figure 7A; it should be noted that the thickness of SnO_2 in these experiments was kept constant at 0.75 μm. As can be seen from the figure, following the deposition of a thin film of TiO_2 ($\sim$0.2 μm) on SnO_2 film, there is clearly an increase in the value of IPCE. This is in accordance with the fact that a better charge separation is occurring in the coupled system. However, as the thickness of TiO_2 film further increases, the IPCE, surprisingly, starts to decrease and approaches a plateau for 1 μm thick TiO_2 films. To ensure us that this decreasing propensity was not due to something adverse inherent in the texture or morphology of thicker TiO_2 film, parallel experiments of the variation in IPCE as a function of thickness of TiO_2 film for simple OTE/TiO_2/Ru(II) system were also performed. Quite the contrary, IPCE continually increases with the increase in TiO_2 thickness although more slowly after the film thickness of 1 μm (Figure 7B). This increase, of course, is understandable in view of the fact that the greater is the adsorption of Ru(II) on thicker TiO_2 film the greater is the LHE of Ru(II) and, hence, larger is the photocurent produced. Thus, the decrease of IPCE with thicker

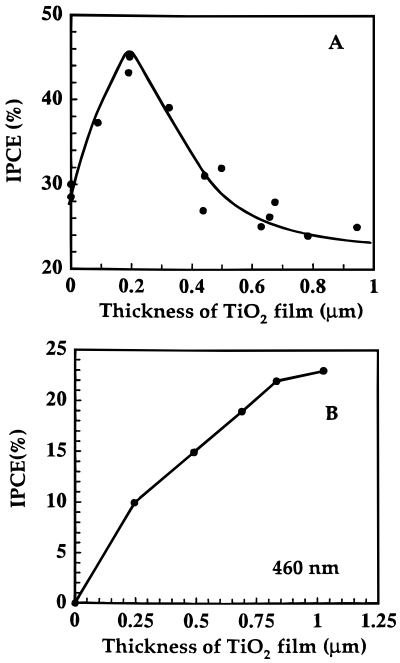

Figure 7. Variation of IPCE at 460 nm with the thickness of TiO_2 film in (A) coupled OTE/SnO_2/TiO_2/Ru(II) system under BF illumination, where the thickness of SnO_2 film was kept constant at 0.75 μm and zero thickness of TiO_2 film refers to OTE/SnO_2/Ru(II), and (B) simple OTE/TiO_2/Ru(II) system (electrolyte: 0.04 M I_2 and 0.5 M LiI in acetonitrile).

films of TiO_2 in the coupled system suggests that there is an optimum thickness of TiO_2 film that yields the best results.

(e) Back Electron Transfer. It has been shown previously that the back electron transfer between the electrons injected in the semiconductor and the oxidized sensitizer is one of the major limiting factors to the efficiency of the cells. Therefore, to improve the operation of the cell, the back reaction 6 must be suppressed.

In the results reported above, it has been demonstrated that the coupling increases the photocurrent generation through better charge separation and lower recombination losses. If, indeed, this is true, it should also manifest itself in the decrease of the back-electron-transfer rate. The electron capture by Ru(III) was monitored by following the recovery of Ru(II) from Ru(III) at 397 nm.[1c,41] No attempt to remove oxygen was made as we are interested in the performance of the systems in ambient conditions. It should, however, be noted that the effect of oxygen on the performance of plain and dye-sensitized TiO_2 has recently been reported by Lindstrom et al.[6] and Rensmo et al.[50]

Figure 8 shows the bleaching recovery at 397 nm for OTE/SnO_2/Ru(II), OTE/TiO_2/Ru(II) and coupled OTE/SnO_2/TiO_2/Ru(II) systems. It should be noted that this wavelength corresponds to the isosbestic point of Ru(II)* and Ru(II) absorption.[1c,41] Therefore, the conversion of Ru(II)* to Ru(III), as a result of charge injection into semiconductor, with $\epsilon_{max,Ru(III)} < \epsilon_{max,Ru(II)*}$, causes a bleaching at 397 nm and yields a negative absorbance change (ΔA). The recovery of this bleaching is, thus, the direct result of electron capture by Ru(III) or the back-electron-transfer reaction 6. The ΔA−time traces (Figure 8) show the back electron transfer to be a multiexponential process and suggest that the heterogeneous electron transfer is controlled by the inhomogeneity of trap and/or surface sites. It should be mentioned that the bleaching recovery was monitored at the same laser intensity for all the systems to avoid the dependence of k_r on excitation intensity.[51−53]

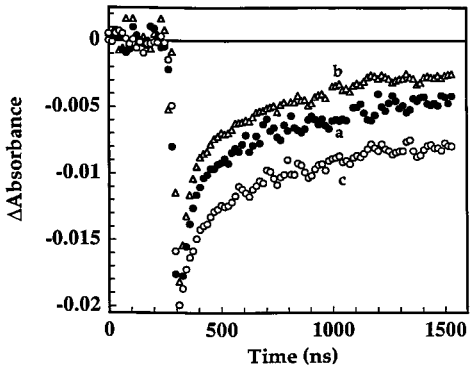

Figure 8. Absorption−time profiles recorded at 397 nm following the 532 nm laser pulse exictation of (a) OTE/SnO_2/Ru(II), (b) OTE/TiO_2/Ru(II), and (c) OTE/SnO_2/TiO_2/Ru(II) systems.

The analysis of the multiexponential decay has been carried out using the stretched exponential kinetic function or Kohlrausch relaxation function,[54−56] the utilization of which has recently been thoroughly discussed by Ford *et al.*[51] Briefly, this function models a system that relaxes with a distribution of exponential decay times whose peak value is close to the characteristic lifetime τ_k. It is described by the following equation:

$$\Delta A(t) = \Delta A_o \exp(-(t/\tau_k)^{\beta}) \quad (7)$$

where $\Delta A(0)$ and $\Delta A(t)$, are respectively the absorbance changes at zero and time t and β is the stretching parameter. The width of the distribution is inversely related to β, i.e., as β increases, the distribution becomes narrower, and at $\beta = 1$, the function describes a monoexponential decay. This function is further characterized by an average lifetime $\langle\tau_k\rangle$:[57−59]

$$\langle\tau_k\rangle = (\tau_k/\beta)\Gamma(\beta^{-1}) \quad (8)$$

where Γ is the gamma function.

To get a more reliable fit over the entire kinetic trace, the bleaching recovery at 397 nm was separately recorded for various time intervals over a period of a 3−4 decades and compiled for the determination of lifetimes as described elsewhere.[46] The values derived for β were in the range of 0.55 to 0.65, suggesting a similar distribution of lifetimes in all the electrodes. Both the characterstic lifetime, τ_k, and average relaxation time, $\langle\tau_k\rangle$, in the present study, correspond to the back-electron-transfer rate. The rate constants, k_r, for simple OTE/TiO_2/Ru(II) and OTE/SnO_2/Ru(II) systems are found to be, respectively, 1.2×10^6 s^{-1} and 2.3×10^6 s^{-1}, while that for the coupled OTE/SnO_2/TiO_2/Ru(II) system is 4×10^5 s^{-1}. This shows a decrease of 3−5 times in the rate of back electron transfer for the coupled system compared to those for the simple ones and provides a supportive evidence for an improved charge separation with the coupled electrode.

(f) Dependence of k_r with Thickness of TiO_2 Film. Similar to the measurements of the variation of IPCE with thickness, the influence of thickness of TiO_2 film on back electron transfer in the coupled OTE/SnO_2/TiO_2/Ru(II) system was also studied. The rate constants k_r for various thicknesses of TiO_2 film were obtained from the recovery of the bleaching at 397 nm as described in the previous section, and the results are presented in Figure 9. Interestingly, the dependence of k_r on the thickness of TiO_2 is just the opposite of that for IPCE (Figure 7A). In fact, following the deposition of a thin film of TiO_2 ($\sim$0.2 μm), we observe a significant decrease in k_r due to a better charge

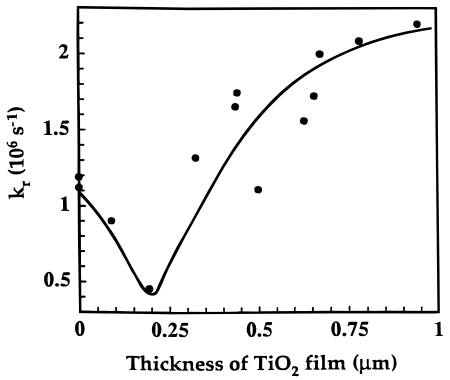

Figure 9. Dependence of back-electron-transfer rate constant, k_r, on thickness of TiO_2 film in the coupled OTE/SnO_2/TiO_2/Ru(II) system.

separation or a slower charge recombination process. However, when the film of TiO_2 becomes thicker, k_r, consistent with the observation of decrease in IPCE, starts increasing and at a thickness of ~1 μm its value reaches that for a simple OTE/TiO_2/Ru(II) system.

Discussion

As mentioned in the Introduction, our primary objective to couple TiO_2 with SnO_2 was to exploit the beneficial role of the coupled electrode in enhancing the process of charge separation in a photoelectrochemical cell based on Ru(II)-modified nanocrystalline semiconductor films. The rationale behind this was that, in view of the conduction band of SnO_2 being at lower energy than that of TiO_2, the photoinjected electrons from Ru(II)* into TiO_2 will quickly be transferred to SnO_2, thus helping photogenerated electrons to escape recombination with holes and thereby improving the charge separation efficiency.

The IPCE measurements, presented in Figure 3, clearly demonstrate an increase in the photoresponse of the coupled OTE/SnO_2/TiO_2/Ru(II) system compared to those for simple OTE/SnO_2/Ru(II) and OTE/TiO_2/Ru(II) ones, proving, therefore, a better charge separation, as a result of quick cascading of electrons from TiO_2 to SnO_2, in the coupled system. Other photoelectrochemical characteristics, namely, higher photovoltage, similar action spectra for FF and BF modes of illumination, suppression in back-electron-transfer rate, and a negligible photocurrent in reverse coupled system, all underscore the importance of the vectorial electron transfer from TiO_2 to SnO_2 and, hence, the potential of the coupled system for better charge separation and improving the performance of a DSPE solar cell.

The results of the variation of IPCE with the thickness of TiO_2 film in the coupled system (Figure 7A), where IPCE initially increases but later decreases as the thickness of TiO_2 film increases, are intriguing but quite interesting and may be understood in terms of a delicate balance between the forces of charge separation and charge recombination processes. The increase in IPCE is, of course, the result of the coupling of SnO_2 with TiO_2. As soon as TiO_2 is deposited on SnO_2, the coupling action is set in motion. The cascade of electrons from TiO_2 to SnO_2 is activated and the electrons injected in TiO_2 from Ru(II)* are driven away from the holes. This enhances the charge separation and reduces the charge recombination losses.

For the coupled OTE/SnO_2/TiO_2/Ru(II) system with thin TiO_2 film, the charge separation dominates the recombination process and leads to an increase in IPCE, and can be visualized as follows. It should be recalled that it is the TiO_2 film which receives the electrons from Ru(II)* first, and the role of SnO_2, with its lower lying conduction band, is merely to provide the beneficial driving force to pull electrons away from TiO_2 and, hence, away from the holes left in Ru(II), to prevent charge recombination. Thus, in the coupled system with thinner TiO_2 films, where charge injection from Ru(II)* into TiO_2 occurs closer to the SnO_2/TiO_2 interface, the photoinjected electrons are able to sense and perceive the pull supplied by the adjacent SnO_2 layer, with the result most of the electrons injected from Ru(II)* into TiO_2 are quickly transferred to SnO_2 particles, leading to an efficient charge separation. Once in SnO_2, the electrons are comparatively farther away from the holes and the charge recombination is less severe. In view of the domination of charge separation over charge recombination, one observes an increase in IPCE.

At this point, a word regarding the total thickness of the semiconductor film and role of LHE of Ru(II) in IPCE is in order. In our earlier work with the sensitization of nanocrystalline ZnO films with Ru(II), it was shown that IPCE increased as ZnO film became thicker.[1b] Similar observations were also made by Liu et al.,[13] who reported that the IPCE of H-aggregates of cresyl violet, adsorbed on a nanocrystalline SnO_2 electrode, increased with the increase in SnO_2 film thickness. These results were explained in terms of increased LHE of the sensitizer adsorbed on thicker semiconductor films. Since thickness of the semiconductor film increases in the coupled electrode and, as a result, LHE of Ru(II) deposited on coupled electrode also increases, one may thus ask the following: Is the increase in IPCE observed in the coupled OTE/SnO_2/TiO_2/Ru(II) system compared to the simple OTE/SnO_2/Ru(II) and OTE/TiO_2/Ru(II) ones really due to the process of better charge separation or rather due to a simple increase of the total thickness of the semiconductor film? This, however, can be ruled out on the following grounds:

First, according to Figure 7A, the IPCE of OTE/SnO_2/Ru(II), i.e., the coupled system with zero thickness of TiO_2 film, is ~28%; the thickness of the SnO_2 film is ~0.75 μm. After depositon of a thin layer of TiO_2 (~0.2 μm), the IPCE of the coupled electrode jumps to 46%, i.e., produces an increase of 50%; the total thickness of the composite semiconductor film is now 1 μm. In separate experiments as mentioned in section IIa, the IPCE of a simple OTE/SnO_2/Ru(II) system showed an increase of ~10%, i.e., remained around 30%, as the thickness of SnO_2 film changed from 0.75 to 1 μm. It is also interesting to note from Figure 7B that the IPCE of a simple OTE/TiO_2/Ru(II) system, also with 1 μm thick TiO_2 film, remains in the vicinity of 22−25%. In other words, a propotionate increase in the thickness of the semiconductor film in simple systems does not really translate into an equivalent increase in IPCE as found in the coupled system.

Second, the increase in LHE of Ru(II) in coupled system, after deposition of the thin (0.2 μm) TiO_2 film on SnO_2 film (inset, Figure 2), as mentioned earlier, is only ~12%, whereas the IPCE of the coupled system shows an increase of about 50 and 100% relative to the OTE/SnO_2/Ru(II) and OTE/TiO_2/Ru(II) systems. The third and far more compelling reason is provided by a very little IPCE observed with the reverse coupled OTE/TiO_2/SnO_2/Ru(II) system in which the total thickness of the semiconductor assembly was even higher than 1 μm (TiO_2, 0.75 μm; SnO_2, = 0.75 μm). Once again, if the increase in IPCE in coupled system was due to the higher thickness of the semiconductor assembly, then a similar higher IPCE (~45%) should have also been obtained with the reverse coupled system, which, however, as seen from the spectrum d in Figure 3, is not the case, even though the uptake of Ru(II) is higher than that for the coupled system. These results, thus, unequivocally

confirm that the augmentation of IPCE seen with the coupled electrode is, indeed, due to the process of enhanced charge separation and not due to a simple case of an increase in the thickness of the semiconductor film and LHE of Ru(II).

As far as the decrease in IPCE at higher thickness of TiO_2 film is concerned, it is the consequence of the increased recombination losses. Contrary to the case of the coupled system with thin TiO_2 films, the charge injection from Ru(II)* in coupled OTE/SnO_2/TiO_2/Ru(II) system with thicker TiO_2 films occurs into the outer layers of TiO_2, farther from the SnO_2/TiO_2 interface. The photoinjected electrons, thus, rather fail to feel the pull of the adjacent SnO_2 layer. As a result, not all the electrons injected from Ru(II)* into TiO_2 are quickly transferred to SnO_2 particles. In fact, in this case, the charges have to first move some distance within the TiO_2 film itself before they can enter a, sort of, "force field" of SnO_2 to be able to be rapidly swept away from the holes. Hence, as the TiO_2 film gets thicker, this distance to be traversed by the photoinjected electrons in the, so-called, "unprotected portion" of the TiO_2 film, bereft of the SnO_2 pull, increases and leaves the electrons to their own fate, i.e., indefensible against and vulnerable to the predatory action of the holes, and becomes the prime source of the increased recombination losses. Consequently, as the thickness of TiO_2 film increases, charge recombination becomes dominant and IPCE declines.

It is, thus, the interplay between the forces of charge separation and charge recombination, modulated by the TiO_2 film thickness, that dictates the successful arrival of the charges at the collecting electrode and is responsible for the observed dependence of IPCE on thickness of TiO_2 film. For effective charge separation, therefore, it is important how close the electrons, injected in the TiO_2 film, are to the SnO_2/TiO_2 interface; the correct thickness of TiO_2 film is, therefore, at the heart of efficient functioning of the coupled OTE/SnO_2/TiO_2/Ru(II) system.

The IPCE data, Figure 7A, show that the best results are obtained with TiO_2 film thickness of 0.2 μm. That is, to reap the full potential of the coupled SnO_2/TiO_2 electrode, in bringing about an efficient charge separation in Ru(II)-based DSPE cell, the optimal thickness of TiO_2 film is around 0.2 μm. Beyond this thickness, the advantageous influence of SnO_2 to pull electrons into it seems to be wanning. In fact, at higher thicknesses, the outer layers of TiO_2 film in the coupled system virtually seem to lose touch with the adjacent SnO_2 layer, and the desired purpose of SnO_2 practically disappears. The coupled system in such a situation simply behaves as a simple OTE/TiO_2/Ru(II) one, totally devoid and deprived of the beneficial aspect of SnO_2. This is clearly visible from the IPCE of the coupled system (Figure 7A), with 1 μm thick TiO_2 film, which approaches the value (25%) for the simple OTE/TiO_2/Ru(II) system with the same thickness of TiO_2 film (Figure 7B). This is further corroborated by the FF and BF action spectra of the coupled system with thick TiO_2 film (Table 1), which follow the trends of the simple OTE/TiO_2/Ru(II) system (Figure 5A), with no vestige of the SnO_2 layer, exhibiting pronounced differences in IPCE for FF and BF illumination in contrast to the similar BF and FF spectra obtained for the coupled system with a thin TiO_2 film (Figure 5B).

This optimal thickness of the TiO_2 film, i.e., the distance from the SnO_2/TiO_2 interface into the TiO_2 film, where there is no impediment to the quick cascading and rapid sweeping of electrons from TiO_2 to SnO_2 resulting in an efficient charge separation, may be viewed as an "active region of charge separation" and seems to be rather reminiscent of the "depletion layer" in polycrystalline cells. However, due to the nanometer size of the particulate films, whether an electric field, similar to that present in the depletion layer, really exists at the SnO_2/TiO_2 interface of the coupled electrode is open to question and cannot be said with certainty at the present time. In any case, this thickness defines the region where electron transport is less susceptible to charge recombination effects. It should be pointed out that in the study of the dependence of recombination losses on thickness of semiconductor film in nanoporous TiO_2 cells, a similar analogy between the optimal thickness of nanocrystalline TiO_2 film and the "zone of effective electron hole separation" in polycrystalline cells has also been put forth by Hagfeldt et al.[19a] However, in their case, this zone referred to the distance into the TiO_2 film from the back OTE contact.

The same reasoning, i.e., the competition between the forces of charge separation and charge recombination, can also be advanced to explain the observed dependence of k_r on film thickness (Figure 9). As before, at lower thickness of TiO_2 film, the charge separation, as a result of cascading of electrons from TiO_2 to SnO_2, is efficient. This diminishes the probability of charge recombination and slows down the back-electron-transfer process, resulting in decrease in k_r. With thickness of TiO_2 film greater than the optimum thickness, the photoinjected electrons, as mentioned earlier, have first to be transported in the "unprotected portion" of the TiO_2 film. This increases the probability of back electron transfer, and consequently, there is preponderance of charge recombination which leads to an increase in the values of k_r. In the extreme case of thick films of TiO_2, the charge recombination completely overwhelmes the beneficial effect of SnO_2, and k_r rises to its maximum value. The coupled system in this case, as observed in the experiments of IPCE vs film thickness, resembles more like a simple OTE/TiO_2/Ru(II), with no memory of the SnO_2 film, as is evident from the similar values of k_r for the two systems with 1 μm thick TiO_2 film (Figure 9 and Table 1). Since the processes of charge separation and charge recombination work in opposite directions, the increase/decrease in k_r is consistent with the decrease/increase in IPCE (Figures 9 and 7A).

In the end, it should be mentioned that the beneficial role of the coupling in decreasing the wasteful charge recombination in dye-sensitized nanocrystalline films has earlier been demonstrated.[21,41] However, the results presented above show that the coupling of two semiconductors would be of no use if the thickness of the semiconductor films is not properly controlled.

Conclusion

The present study shows that the coupled semiconductor electrode can bring about an efficient charge separation in nanoporous dye sensitized photoelectrochemical solar cells. The increased IPCE, higher photovoltage, and lower back-electron-transfer rate, k_r, in the coupled OTE/SnO_2/TiO_2/Ru(II) system compared to those for simple OTE/TiO_2/Ru(II) and OTE/SnO_2/Ru(II) ones do testify to the potential of the coupled SnO_2/TiO_2 electrode in improving the performance of a ruthenium complex based nanocrystalline photoelectrochemical cell. A negligible photoresponse with the reverse coupled OTE/TiO_2/SnO_2/Ru(II) system further emphasizes the crucial role of the proper placement of the energy levels of the semiconductor components, in the coupled semiconductor assembly, in vectorial electron transfer for efficient charge separation.

The variation of IPCE (and k_r) in the coupled OTE/SnO_2/TiO_2/Ru(II) system, which shows an initial increase (decrease) in IPCE (k_r) but a subsequent decrease (increase) as the thickness of TiO_2 film further increases, suggests a delicate balance

between the processes of charge separation and charge recombination and underlines the importance of optimum thickness of the nanocrystalline films in reaping the full potential of the coupled electrode. The results show that while coupling of the semiconductors can be beneficial and may provide a simple alternative to minimize the back electron transfer, one should, however, in the pursuit of exploring these coupled systems, bear in mind the primordial effect of the semiconductor thickness on the global performance of the coupled photoelectrochemical cell.

Acknowledgment. We thank Dr. B. Gregg for giving us a detailed description for the preparation of TiO_2 colloids and Mr. K. Jacobson for helping us with the thickness measurements. The work described herein was supported by the Natural Sciences and Engineering Research Council of Canada (C.N. and S.H.) and by the Office of the Basic Energy Sciences of the U.S. Department of Energy (P.V.K.). C.N. is also grateful to Ministère de l'Éducation Nationale du Maroc for a fellowship and for a partial financial support from Radiation Laboratory. This is a contribution No. 4080 from the Notre Dame Radiation Laboratory.

References and Notes

(1) (a) Bedja, I.; Hotchandani, S.; Kamat, P. V. *J. Phys. Chem.* **1994**, *98*, 4133−4140. (b) Bedja, I.; Kamat, P. V.; Hua, X.; Lappin, A. G., Hotchandani, S. *Langmuir* **1997**, *13*, 2398−2403. (c) Kamat, P. V.; Bedja, I.; Hotchandani, S.; Patterson, L. K. *J. Phys. Chem.* **1996**, *100*, 4900−4908.

(2) Meyer, G. J.; Searson, P. C. *Interface* **1993**, 23−27. (b) Cao, F.; Oskam, G.; Meyer, G. J.; Searson, P. C. *J. Phys. Chem.* **1996**, *100*, 17021−17027.

(3) Murakoshi, K.; Kano, G.; Wada, Y.; Yanagida, S.; Miyazaki, H.; Matsumoto, M.; Murasawa, S. *J. Electroanal. Chem.* **1995**, *396*, 27−34.

(4) (a) O'Regan, B.; Graetzel, M. *Nature (London)* **1991**, *353*, 737−740. (b) Nazeeruddin, M. K.; Kay, A.; Rodicio, I.; Humphry-Baker, R.; Mueller, E.; Liska, P.; Vlachopoulos, N.; Gratzel, M. *J. Am. Chem. Soc.* **1993**, *115*, 6382−6390.

(5) (a) Argazzi, R.; Bignozzi, C. A.; Heimer, T. A.; Castellano, F. N.; Meyer, G. J. *Inorg. Chem.* **1994**, *33*, 5741−5749. (b) Heimer, T. A.; Bignozzi, C. A.; Meyer, G. J. *J. Phys. Chem.* **1993**, *97*, 11987-11994. (c) Argazzi, R.; Bignozzi, C. A.; Heimer, T. A.; Castellano, F. N.; Meyer, G. J. *J. Phys. Chem. B* **1997**, *101*, 2591−2597.

(6) Lindstrom, H.; Rensmo, H.; Sodergren, S.; Solbrand, A.; Lindquist, S. *J. Phys. Chem.* **1996**, *100*, 3084−3088.

(7) (a) Redmond, G.; Fitzmaurice, D.; Graetzel, M. *Chem. Mater.* **1994**, *6*, 686−691. (b) Hoyle, R.; Sotomayer, J.; Will, G.; Fitzmaurice, D. *J. Phys. Chem. B* **1997**, *101*, 10791−10800.

(8) (a) Nasr, C.; Hotchandani, S.; Kamat, P. V.; Das, S.; George Thomas, K.; George, M. V. *Langmuir* **1995**, *11*, 1777−1783. (b) Bedja, I.; Hotchandani, S.; Carpentier, R.; Fessenden, R. W.; Kamat, P. V. *J. Appl. Phys.* **1994**, *75*, 5444−5456. (c) Bedja, I.; Kamat, P. V.; Hotchandani, S. *J. Appl. Phys.* **1996**, *80*, 4637−4643. (d) Nasr, C.; Liu, D.; Hotchandani, S.; Kamat, P. V. *J. Phys. Chem.* **1996**, *100*, 11054−11061.

(9) (a) Kay, A.; Graetzel, M. *J. Phys. Chem.* **1993**, *97*, 6272−7. (b) Kay, A.; Humphry-Baker, R.; Graetzel, M. *J. Phys. Chem.* **1994**, *98*, 952−959. (c) Enea, O.; Moser, J.; Graetzel, M. *J. Electroanal Chem.* **1989**, *259*, 59−65.

(10) (a) Tennakone, K.; Kumara, G. R. R. R.; Kumarasinghe, A. R.; Wijayantha, K. G. U.; Sirimanne, P. M. *Semicond. Sci. Technol.* **1995**, *10*, 1689−1693.; (b) Tennakone, K.; Kumarasinghe, A. R.; Sirimanne, P. M. *Semicon. Sci. Technol.* **1993**, *8*, 1557−1560.; (c) Tennakone, K.; Kumara, G. R. R. R.; Kottegoda, I. R. M.; Wijayantha, K. G. U. *Semicond. Sci. Technol.* **1997**, *12*, 128−132.

(11) O'Regan, B.; Schwartz, D. T. *Chem. Mater.* **1995**, *7*, 1349−1354.

(12) Ferrere, S.; Zaban, Arie.; Gregg, B. A. *J. Phys. Chem. B* **1997**, *100*, 4490−4493.

(13) (a) Liu, D.; Kamat, P. V. *J. Electrochem. Soc.* **1995**, *142*, 835−839. (b) Liu, D.; Hug, G. L.; Kamat, P. V. *J. Phys. Chem.* **1995**, *99*, 16768−16775.

(14) Lampert, C. M. *Solar Energy Mater. Solar Cells* **1994**, *32*, 307−321.

(15) Kamat, P. V. *Chem. Rev.* **1993**, *93*, 267−300.

(16) Hagfeldt, A.; Graetzel, M. *Chem. Rev.* **1995**, *95*, 49−68.

(17) Curran, J. S.; Lamouche, D. *J. Phys. Chem.* **1983**, *87*, 5405−5411.

(18) O'Regan, B.; Moser, J.; Anderson, M.; Graetzel, M. *J. Phys. Chem.* **1990**, *94*, 8720−8726.

(19) (a) Hagfeldt, A.; Bjorksten, U.; Lindquist, S. E. *Sol. Energy Mater. Sol. Cells* **1992**, *27*, 293−304. (b) Södergren, S.; Hagfeldt, A.; Olsson, J.; Lindquist, S.-E. *J. Phys. Chem.* **1994**, *98*, 5552−5556.

(20) Albery, W.; Bartlett, P. N. *J. Electrochem. Soc.* **1984**, *131*, 315−320.

(21) Hotchandani, S.; Kamat, P. V. *J. Phys. Chem.* **1992**, *96*, 6834−6839.

(22) Gopidas, K. R.; Bohorquez, M.; Kamat, P. V. *J. Phys. Chem.* **1990**, *94*, 6435−6440.

(23) (a) Spanhel, L.; Henglein, A.; Weller, H. *Ber. Bunsen-Ges. Phys. Chem.* **1987**, *91*, 1359−1363. (b) Spanhel, L.; Weller, H.; Henglein, A. *J. Am. Chem. Soc.* **1987**, *109*, 6632−9635.

(24) Weller, H. *Ber. Bunsen-Ges. Phys. Chem.* **1991**, *95*, 1361−1365.

(25) Vogel, R.; Pohl, K.; Weller, H. *Chem. Phys. Lett.* **1990**, *174*, 241−246.

(26) Gerischer, H.; Luebke, M. *J. Electroanal. Chem. Interfacial Electrochem* **1986**, *204*, 225−227.

(27) Kohtani, S.; Kudo, A.; Sakata, T. *Chem. Phys. Lett.* **1993**, *206*, 166−170.

(28) (a) Liu, D.; Kamat, P. V. *J. Phys. Chem.* **1993**, *97*, 10769-10773. (b) Liu, D.; Kamat, P. V. *J. Electroanal. Chem. Interfacial Electrochem* **1993**, *347*, 451−456.

(29) Nasr, C.; Kamat, P. V.; Hotchandani, S. *J. Electroanal. Chem.* **1997**, *420*, 201−207.

(30) Vogel, R.; Hoyer, P.; Weller, H. *J. Phys. Chem.* **1994**, *98*, 3183−3188.

(31) Evans, J. E.; Springer, K. W.; Zhang, J. Z. *J. Chem. Phys.* **1994**, *101*, 6222−6225.

(32) Hotchandani, S.; Kamat, P. V. *Chem. Phys. Lett.* **1992**, *191*, 320−326.

(33) (a) Vinodgopal, K.; Bedja, I.; Kamat, P. V. *Chem. Mater.* **1996**, *8*, 2180−2187. (b) Vinodgopal, K.; Kamat, P. V. *Environ. Sci. Technol.* **1995**, *29*, 841−845.

(34) Serpone, N.; Borgarello, E.; Graetzel, M. *J. Chem. Soc., Chem. Commun.* **1984**, 342−343.

(35) Serpone, N.; Maruthamuthu, P.; Pichat, P.; Pelizzetti, E.; Hidaka, H. *J. Photochem. Photobiol., A: Chem.* **1995**, *85*, 247−255.

(36) Tennakone, K.; Iieperuma, O. A.; Bandara, J. M. S.; Kiridena, W. C. B. *Semicond. Sci. Technol.* **1992**, *7*, 423−424.

(37) Papp, J.; Soled, S.; Dwight, K.; Wold, A. *Chem. Mater.* **1994**, *6*, 496−500.

(38) Anderson, C.; Bard, A. J. *J. Phys. Chem.* **1995**, *99*, 9882−9885.

(39) Fu, X.; Clark, L. A.; Yang, Q.; Anderson, M. A. *Environ. Sci. Technol.* **1996**, *30*, 647−653.

(40) Torimoto, T.; Fox, R. J., III; Fox, M. A. *J. Electrochem. Soc.* **1996**, *143*, 3712−3717.

(41) Nasr, C.; Hotchandani, S.; Kim, W. Y.; Schmehl, R. H.; Kamat, P. V. *J. Phys. Chem. B* **1997**, *101*, 7480−7487.

(42) Fessenden, R. W.; Kamat, P. V. *J. Phys. Chem.* **1995**, *99*, 12902−12906.

(43) Bedja, I.; Hotchandani, S.; Kamat, P. V. *Ber. Bunsen-Ges. Phys. Chem.* **1997**, *101*, 1651−1653.

(44) Zaban, A.; Ferrere, S.; Sprague, J.; Gregg, B. A. *J. Phys. Chem. B* **1997**, *101*, 55−57.

(45) Nagarajan, V.; Fessenden, R. W. *J. Phys. Chem.* **1985**, *89*, 2330−2335.

(46) Nasr, C.; Hotchandani, S.; Kamat, P. V. *J. Phys. Chem. B* **1998**, *102*, 4944−4951.

(47) Hodes, G.; Howell, I. D. J.; Peter, L. M. *J. Electrochem. Soc.* **1992**, *139*, 3136−40.

(48) Alonso-Vante, N.; Nierengarten, J. F.; Sauvage, J. P. *J. Chem. Soc., Dalton Trans.* **1994**, *11*, 1649−1654.

(49) Bard, A. J.; Parsons, R.; Jordan, J. *Standard Potentials in Aqueous Solution*; Marcel Dekker: New York, 1985.

(50) Rensmo, H.; Lindstrom, H.; Sodergren, S.; Willstedt, A.-K.; Solbrand, A.; Hagfeldt, A.; Lindquist, S. E. *J. Electroanal. Chem.* **1996**, *143*, 3173−3178.

(51) Ford, W. E.; Wessels, J. M.; Rodgers, M. A. J. *J. Phys. Chem. B* **1997**, *101*, 7435−7442.

(52) Liu, D.; Fessenden, R. W.; Hug, G. L.; Kamat, P. V. *J. Phys. Chem. B* **1997**, *101*, 2583−2590.

(53) Haque, S. A.; Tachibana, Y.; Klug, D. R.; Durrant, J. R. *J. Phys. Chem. B* **1998**, *102*, 1745−1749.

(54) Plonka, A. *Time dependent reactivity of species in condensed media*; Springer-Verlag: New York, 1986.

(55) Siebrand, W.; Wildman, T. *Acc. Chem. Res.* **1986**, *19*, 238−243.

(56) Richert, R. *Chem. Phys. Lett.* **1985**, *118*, 534−538.

(57) Linsey, C. P.; Patterson, G. D. *J. Chem. Phys.* **1980**, *73*, 3348−3357.

(58) Leung, L. K.; Komplin, N. J.; Ellis, A. B.; Tabatabaie, N. *J. Phys. Chem.* **1991**, *95*, 5918−5924.

(59) Ford, W. E.; Rodgers, M. A. J. *J. Phys. Chem. B* **1997**, *101*, 930−936.